

## **3D connectivity of eutectic Si as a key property defining strength of Al-Si alloys**

A. Kruglova<sup>a</sup>, M. Engstler<sup>a</sup>, G. Gaiselmann<sup>b</sup>, O. Stenzel<sup>b</sup>, V. Schmidt<sup>b</sup>, M. Roland<sup>c</sup>, S. Diebels<sup>c</sup>, F. Mücklich<sup>a</sup>

<sup>a</sup> Chair of Functional Materials, Saarland University, D-66123 Saarbrücken, Germany

<sup>b</sup> Institute of Stochastics, Ulm University, D-89069 Ulm, Germany

<sup>c</sup> Chair of Applied Mechanics, Saarland University, D-66123 Saarbrücken, Germany

### **Abstract**

The relationship between microstructure and mechanical behavior of the eutectic phase in hypoeutectic Al-Si alloys is analyzed empirically using two experimental and thirteen synthetic microstructures. For all microstructures, a morphological analysis is combined with mechanical stress-strain simulations performed via finite element method (FEM). The synthetic microstructures are generated by a stochastic microstructure model that gives a realistic description of the eutectic Si in Al-Si alloys. The stochastic model was developed on the basis of a 3D image of a real Sr-modified Al-Si alloy and is used to generate a large variety of virtual 3D structures of eutectic Si that differ from each other by the number of Si particles, their degree of branching, and connectivity. In the simulation study, it is shown that highly connected and branched morphologies of Si are beneficial to the strength of the material. Besides, when the connectivity of Si is low, i.e. when an Al matrix is reinforced by discrete (disconnected) particles of Si, the strength of the material increases with the

number of those particles. The Euler number is shown to be highly effective in characterizing the connectivity and is closely related to the strength of the material.

**Keywords:** Al-Si alloys; microstructure; computer simulations; mechanical properties; connectivity

## 1. Introduction

Nowadays, Al-Si castings are widely used in the production of automobile parts. In particular, a hypoeutectic composition (<12 wt.% Si) of the material provides a good castability and corrosion resistance. The tensile strength and ductility of these alloys can be improved through the modification of the eutectic by adding small amounts of modifiers, such as Na or Sr [1–3]. There are numerous publications studying the topic of eutectic modification and its influence on the mechanical properties of the alloy [1,4–6]. Modified Si particles usually have a fine fibrous morphology [7], also denoted as coral-like morphology in this paper, see Fig. 1a. To clarify notation, in this paper, we denote every single disconnected volume of Si as “particle” (i.e. two particles are always disconnected) and its subcomponents as “branches”.

In general, the mechanical behavior of Al-Si alloys is mainly defined by the 3D architecture, i.e. the morphology and spatial arrangement of the Si particles within the Al-Si eutectic. A network of stiff Si particles in a ductile Al matrix increases the strength of the material while decreasing its ductility [8–9]. A connected brittle phase (as the eutectic Si) also facilitates the crack propagation [4]. Thus, the connectivity of the eutectic Si, among other morphological properties, strongly influences the mechanical properties of the alloy.

The effect of the connectivity of a rigid phase (silicon or other reinforcement) on the strength of different Al-Si-based alloys has been presented in [9]. In this context, the Al-Si alloy can be regarded as a metal matrix composite with the eutectic Si as a strengthening phase [10]. The unmodified AlSi12 alloy with interconnected Si lamellae has shown an increase in strength and work hardening compared to the same alloy after a solution treatment at 540 °C for 4h, which leads to a disintegration of the lamellae and a loss of interconnections between the particles [8]. The strengthening effect of Si is due to the load transfer from the Al matrix to the Si and the difference in thermal expansion coefficients between the components, resulting in strain-hardened regions around the Si during the cooling process. The stiff Si network interpenetrating the ductile Al matrix increases the load transfer from the matrix to the reinforcement and thus enhances the strength. On the contrary, the disintegration of the network due to the heat treatment has an adverse effect on the strength, although it is beneficial to the ductility [9].

Until recently, the study of the relation between the silicon morphology and mechanical properties of Al-Si alloys has been limited to 2D investigations in most cases [11–12]. However, characteristics such as connectivity, particle density, and other basic characteristics can only be determined in 3D [13], for example with the help of tomographic imaging techniques. Particularly, focused ion beam/scanning electron microscopy (FIB/SEM) tomography is suitable to reveal the 3D architecture of the eutectic Si with a high resolution. In [14], this technique has been used for the reconstruction of the Al-Si eutectic in an AlSi12(Sr) alloy with a spatial resolution of  $10^{-4}$  to  $10^{-3} \mu\text{m}^3$ . On the other hand,

the 3D FIB/SEM imaging technique is costly and time-consuming and the morphology of the sampled structure is hardly predictable before analyzed in a destructive nature.

To overcome these disadvantages, a new in-silico approach has been developed to generate virtual but realistic 3D structures of eutectic Si using spatial stochastic modeling [15]. In general, 3D stochastic morphology models use tools from stochastic geometry to generate random 3D morphologies. They have the advantage of generating a large variety of virtual 3D morphologies in a cost and time efficient way. Moreover, one can systematically adjust the morphological properties making stochastic morphology modeling an interesting tool to analyze morphology-functionality relationships when combined with numerical simulations [16]. In the last years, numerous stochastic models have been developed for applications in materials science, ranging from organic solar cells and batteries to fuel cells [17]. For the microstructure of Al-Si eutectic, a stochastic 3D microstructure model was built using methods from stochastic geometry and multivariate time series. It has been fitted to experimental 3D FIB/SEM data (see Fig. 1a) such that the difference between morphological characteristics of the Si particles, like connectivity, particle density etc., in the real and in the virtually generated samples is minimized. The model has proved to reflect the mechanical properties of the eutectic by comparing the results of FEM simulations on both real and virtual samples. Additionally, it has been shown that the mechanical strength simulations are sensitive to the variations of morphological features [18]. Such an in-silico approach can accelerate the research while simultaneously reducing costs. Stochastic simulation models are

capable of generating a large variety of realistic 3D microstructures in a relatively short computational time. Numerical simulations can be performed on these structures to predict their functionality. Subsequently, the outputs of the numerical simulations are analyzed, evaluated and correlated with the corresponding morphological features. Thus, stochastic models can help to elucidate the correlation between the 3D microstructure and functional properties.

This paper describes the effect of connectivity and other related morphological properties of the eutectic Si, such as the degree of branching and the number of particles, on mechanical behavior of the alloy. In particular, a simulation study is performed where thirteen virtual microstructures generated by varying the parameters of the stochastic model are analyzed in terms of both morphological and mechanical properties. In particular, FEM simulations are used to evaluate the mechanical behavior of the virtual structures in terms of mechanical strength. It turns out that the strength of the material increases with the connectivity and the branching of the Si particles as well as with the number of particles for simply connected structures. Furthermore, the strength of the materials increases with decreasing the Euler number, which is a topological characteristic. The microstructures with similar values of the Euler number have a similar mechanical behavior. Thus, the Euler number is a relative, yet effective measure of the strength which allows to compare a performance of different structures without mechanical tests. The results are of great importance for industrial quality control and the development of advanced Al-Si alloys for applications in the automotive industry.

## 2. Materials and Methods

Section 2.1 presents the experimental samples that were used to compare the mechanical behavior of experimental structures with results obtained for the virtual samples. Section 2.2 shortly describes the competitive stochastic growth model (CSGM) for the simulation of the eutectic Si in the Al-Si alloys introduced in [15]. The FEM procedure used for the simulation of the mechanical behavior of the virtual structures is presented in Section 2.3. Finally, the parameters used for the quantitative characterization of the simulated structures are described in Section 2.4.

### *2.1. Experimental data*

The mechanical behavior of two different Sr-modified Al-Si alloys produced by directional solidification and die casting was previously studied in [19]. The 3D Si structure of the castings is shown in Fig. 1; the chemical composition of the castings and the Euler number density are given in Table 1. Note that the Euler number represents the difference between the number of particles in the structure and the connectivity. The Euler number density is simply the Euler number divided by the volume of the bounding box. For a detailed description of 3D image pre-processing and FEM simulations on the reconstructed experimental data of Al-Si alloys, see [19].

Experimental sample no. 1 (Fig. 1a) consists of many disconnected Si particles. It serves as a prototype for the stochastic model. Experimental sample no. 2 (Fig. 1b) comprises Si, most of which merge together and form a network, i.e. a single Si particle. It illustrates the behavior of a structure that has a high connectivity of Si [19].

## *2.2. Competitive stochastic growth model for eutectic Si in Al-Si alloys*

In order to elucidate microstructure properties of the eutectic in Al-Si alloys, CSGM introduced in [15] is used to generate virtual Al-Si alloys with various structural properties. Recall that Al-Si alloys obtained by directional solidification are characterized by a system of pairwise disconnected 3D corals or particles of Si, respectively. The stochastic model was designed to capture this property of disconnectedness by using the following two-stage approach. In the first step, a random spatial graph representing the “skeleton” of eutectic Si is modeled (see Fig. 2). It serves as “backbone” of the disconnected Si particles. The graph structure allows to control the distances between neighboring particles and can therefore adjust the number of disconnected particles. In the second step, volume is added to the graph structure by dilating (“blowing up”) the individual edges of the graph. For this step, two variants are considered:

Variant 1: Each edge of the graph is individually dilated by a centered sphere as the structuring element, for which the corresponding radii are chosen so that a) the desired volume fraction of Si is matched, and b) particles disconnected in their graph structure remain disconnected after the dilation.

Variant 2: All edges are dilated by a centered sphere with a constant radius so that a) the desired volume fraction of Si is matched. Particles disconnected in their graph structure can merge together by the dilation.

Generally, this stochastic morphology model allows to generate random 3D morphologies with different structural properties depending on the values of the model parameters (see Fig 2). The most important parameters for the graph are the following:

- $t_{internal}$  is a parameter related to the minimum distance between edges belonging to the same particle and controls the degree of branching.
- $t_{external}$  is the minimum distance between any two edges from two disconnected particles.
- $r_{cox}$  is related to the minimum distance between two starting points for two disjoint particles and has an influence on the number of particles.

In [15], this stochastic model has been applied to describe the microstructure of the eutectic Si in Sr-modified Al-Si alloys. This means that the values of the model parameters are chosen to achieve the highest parity between experimental and simulated microstructures with respect to important structural characteristics. The fitted model parameters are given by  $t_{internal} = 30$  voxels,  $t_{external} = 20$  voxels, and  $r_{cox} = 55$  voxels. The experimental structure and its virtual counterpart are shown in Fig. 3. For more information about the model and its application to eutectic Si, see [15] [18].

### *2.3. Mechanical simulations*

All virtual microstructures generated by the stochastic model are part of a series of 357 single 2D images, which are merged into a 3D volume mesh, in which the material properties are linearly mapped on the barycenter of each voxel with a size of  $46 \times 46 \times 46 \text{ nm}^3$ . To reduce memory consumption and to accelerate the computations, the meshes have been coarsened by an algorithm that uses a uniform scaling with a simple boxfilter of a variable size with respect to the volume fractions of the particular materials and their mechanical properties. For more details on the coarsening process and the setup of the numerical simulations, see [18].

The material properties of the simulated Al-Si alloys with different Si morphologies are chosen as follows: a Young's modulus of  $E = 70$  GPa, Poisson's ratio of  $\nu = 0.34$ , and yield strength of  $\sigma_y = 40$  MPa are used for the Al, while a Young's modulus of  $E = 107$  GPa, Poisson's ratio of  $\nu = 0.27$ , and yield strength of  $\sigma_y = 7$  GPa are used for the Si. The numerical simulations are realized using the structural mechanics module of COMSOL Multiphysics and an elasto-plastic material model combined with an isotropic hardening [20] [21]. All presented finite element simulations have been done with quadratic Lagrange elements. The numerical simulations of the deformation of different Al-Si alloys have been realized with the following boundary conditions: For every spatial direction, the displacement has been fixed on one side of the mesh and a load curve has been applied to the opposite side. After running each simulation, a stress-strain curve has been computed using the numerical integration of the displacement field in the corresponding spatial direction.

#### *2.4. Quantitative characterization*

Quantitative characteristics of Si, such as the Euler number, the number of particles, their volume as well as the number of branches are computed with the help of Modular Algorithms for Volume Images (MAVI) [22] and the image processing package Fiji [23]. These software tools are specialized in the quantitative geometric analysis of 2D and 3D image data representing microstructures.

Roughly speaking, the connectivity reflects the number of connections between the constituents in a 3D image [24]. For complex structures, it can be characterized in different ways. Tolnai et al. [25] uses the volume fraction of the

largest single particle within the analyzed component as a measure of the interconnectivity. Here, the ratio ( $V_{MaxParticle}/V_{TotalSi}$ ) stands for the volume fraction of the largest Si particle in relation to the total volume occupied by the Si within a bounding box.

The connectivity of the component can also be evaluated by means of the Euler number. The Euler number represents the difference between the number of particles in the structure and the connectivity. Thus, the connectivity is computed by simply subtracting the Euler number from the number of Si clusters. For disconnected particles (the connectivity is 0), the Euler number equals the mean number of particles; and for objects forming a strongly connected network (the connectivity is very high), the Euler number is negative. But in contrast to the previous estimation of the connectivity by means of the volume fraction of the largest particle, the Euler number provides additional information on the topological properties of the structure. Particularly, the Euler number reflects the relation between different types of surface elements presented in the structure such as convex, concave, and saddle surfaces, which correspond to convex particles, holes, and tunnels, respectively [24].

All morphological characteristics are given in absolute values as the volume is the same for all simulated microstructures. Only the Euler number is computed as density (i.e. Euler number density) to be able to compare it with the experimental samples which have a different volume.

### **3. Results and Discussion**

The following section presents the results of the simulation study, where virtually generated microstructures of eutectic Si in Al-Si alloys are first

analyzed by morphological characteristics and subsequently their mechanical behavior is computed by FEM simulations.

This section is divided into three parts: Section 3.1 describes the influence of connectivity and branching on mechanical properties; Section 3.2 analyzes the influence of the number of Si particles on mechanical properties; and finally, Section 3.3 summarizes the influence of the presented morphological characteristics on the mechanical behavior and gives an outlook on the possible future work.

For Section 3.1, variant 2 of the stochastic model is considered; this variant allows to vary the connectivity. In contrast, in Section 3.2 only the influence of the number of Si particles is investigated and, therefore, the connectivity has to be preserved by applying variant 1 of the stochastic model.

### *3.1. Influence of connectivity and degree of branching of particles*

In this section, the influence of the connectivity and the degree of branching of Si particles on the material strength is investigated by generating and analyzing nine virtual microstructures that have varying degrees of connectivity and branching. Note that branching and connectivity go hand in hand, wherefore the effect of branching and connectivity is analyzed simultaneously. The reason for this lies in the stochastic model. Decreasing a competition parameter ( $t_{external}$  or  $t_{internal}$ ) leads to higher branching and lower distances between branches. This increases the chance that they come very close to each other and merge together after the dilation (variant 2) of the simulated tree-like graph structure. Thus, a higher branching of Si particles results in increased connectivity.

The connectivity and the branching of particles are controlled via the external and internal competition parameters  $t_{external}$  and  $t_{internal}$ . Five virtual microstructures are generated by varying  $t_{external}$  and four by varying  $t_{internal}$ . Variations of the external and internal competition parameters are analyzed separately. The third important model parameter  $r_{cox}$  is fixed at  $r_{cox} = 55$  voxels (fitted value of this parameter, cf. Sec. 2.2.) for all virtual microstructures. First, the parameter  $t_{external}$  is varied between 0.1 and 40 voxels while the parameter  $t_{internal}$  is set to 30 voxels (fitted value of this parameter, cf. Sec. 2.2.). Fig. 4 illustrates two extreme cases, one for  $t_{external}$  equal to 0.1 voxels and 40 voxels, respectively. Note that all remaining parameters (which are not listed here) are set equal to the model fitted to experimental sample no. 1. Morphological characteristics of the virtual microstructures are given in Table 2.

As can be seen in Fig. 4 and Table 2, decreasing  $t_{external}$  results in an increase in the volume fraction of the largest individual particle of Si and the number of branches and in a decrease in the number of particles and the Euler number. Due to the reduced external competition parameter, there is more space for branches to appear and to grow in-between neighboring particles: for instance, sample no. 5 has nearly 6 times more branches than sample no. 1. These complementary branches form new connections when filling the space and merging together after the dilation of the graph structure. As some particles merge together, the number of particles decreases and the volume of the largest particle increases: from 3% in sample no. 1 up to 98% in sample no. 5. Clusters in sample no. 1 (Fig. 4b) remain separated, whereas in sample no. 5 (Fig. 4a), there is only one large and highly connected Si particle in the center of

the bounding box and several significantly smaller particles along the volume's edges, which are either cropped parts of the same particle or of any other large particle. Furthermore, the Euler number gets negative indicating thereby an increase in connectivity and the presence of a network structure.

The influence of morphological changes on the mechanical behavior of the structures has been analyzed by comparing simulated stress-strain curves. Fig. 5 shows stress-strain curves obtained by means of FEM simulations for the virtual microstructures and for the two experimental samples. Since all structures have shown nearly the same behavior in the elastic region, Fig. 5 zooms in particularly on the plastic region, where the main difference in mechanical behavior appears. It can be easily seen that the strength of the virtual samples increases with a decreasing  $t_{external}$  and hence, with an increasing connectivity and branching of Si particles.

Experimental sample no. 2 shows the highest strength as well as the most negative Euler number density:  $-2.61 \times 10^{17} \text{ m}^{-3}$  against  $-9.00 \times 10^{16} \text{ m}^{-3}$  for the most high-strength virtual sample no. 5. Experimental sample no. 1 has a positive value of the Euler number density equal to  $4.80 \times 10^{14} \text{ m}^{-3}$ . Therefore, a stress-strain curve of experimental sample no. 1 below the others would be expected. However, this is not the case. The behavior of experimental sample no. 1 is similar to samples no. 2, 3, and 4, but its strength is slightly overestimated due to the synthetically increased volume fraction of Si obtained as a result of a manual segmentation of the experimental images in contrast to the volume fraction of Si that is precisely matched in the virtual samples.

In the next part of the simulation study, the parameter  $t_{internal}$  is varied between 10 and 30 voxels (fitted value of this parameter, cf. Sec. 2.2.). As shown in Fig. 5, experimental sample no. 1 has exactly the same behavior as sample no. 4 with the parameters  $t_{internal}$  equal to 30 voxels and  $t_{external}$  equal to 5 voxels. Thus, we fix the parameter  $t_{external}$  to 5 voxels. In that case, the chosen value of the parameter  $t_{external}$  leads to the formation of network structures in all virtual microstructures since the dilation radius used for most of the simulations is slightly higher than the value of  $t_{external}$  used for building the graph structure (prior to the dilation). Thus, after the dilation of the graph, many new connections are formed. In short, fixing  $t_{external}$  at 5 voxels yields highly connected microstructure which allows to analyze solely the effect of the degree of branching. Fig. 6 shows two extreme cases, one for  $t_{internal}$  equal to 10 voxels and 30 voxels, respectively. Quantitative characteristics of the simulated structures are listed in Table 3.

All structures are characterized by negative Euler numbers which indicates a network geometry. Analogous to the virtual microstructure in Fig. 4a, they consist of a large particle in the center of the virtual microstructure, which comprises over 90% of the Si within the bounding box, and several particles along the sample's edges. The number of particles in Table 3 accounts mostly for those particles that are located along the edges of the bounding box; therefore, it is not relevant in this case. As for  $t_{external}$ , smaller values of  $t_{internal}$  lead to more space for new branches to be formed and to grow, building new connections: for example, sample no. 9 has nearly 3 times more branches and a 6 times higher Euler number density than sample no. 4.

By carrying out FEM simulations on the virtual structures with various internal competition parameters, a behavior similar to that of the structures with different external competition parameters can be observed (see Fig. 7). This is, however, not surprising, since decreasing both parameters results in an increased connectivity. Similar to the previous case, a certain discrepancy appears during plastic deformation. Even if all structures show a high connectivity of the Si particles, which in itself implies a higher strength, the branching of the clusters does have an important influence. The connectivity and the branching of Si particles increase the strength of the material.

The stress-strain curve of experimental sample no. 2 partially overlaps with the curve of sample no. 9. Interestingly, both samples have a quite similar Euler number density:  $-2.61 \times 10^{17} \text{ m}^{-3}$  for experimental sample no. 2 against  $-2.88 \times 10^{17} \text{ m}^{-3}$  for sample no. 9, but correspond to different alloys. The stress-strain curve of experimental sample no. 1 with a positive Euler number density overlaps with the curve of sample no. 4; however, as has been mentioned before, the strength of experimental sample no. 1 has been slightly overestimated due to the increased volume fraction of Si.

### *3.2. Influence of number of particles in simply connected structures*

In this section, the influence of the number of Si particles on the material strength is analyzed. The external and internal competition parameters are chosen such that they preserve the connectivity of the particles, i.e. the neighboring particles separated in their graph structures also remain separated after the dilation. To vary the number of particles, the parameter  $r_{\text{cox}}$  varies between 55 (fitted value of this parameter, cf. Sec. 2.2.) and 120 voxels, which

results in 211 (see Fig. 3b) and 69 clusters (see Fig. 8), respectively.

Corresponding quantitative characteristics are given in Table 4.

Table 4 shows that an increase in the parameter  $r_{cox}$  corresponds to a decrease in the number of particles, since  $r_{cox}$  controls the density of particles in the stochastic model. At the same time, the number of branches per single particle increases. The volume fractions of the largest Si particle as well as the connectivity of particles remain (merely) constant for all samples. This means that the effect of the connectivity on the mechanical behavior can be neglected and the main difference in the behavior of the samples is mainly determined by the number of particles.

By applying FEM simulations to the virtual microstructures with various values of  $r_{cox}$ , as in the previous section, a similar behavior in the elastic region and a discrepancy in the course of plastic deformation can be observed (see Fig. 9). The strength of the material increases with the number of particles. However, microstructures with  $r_{cox}$  of more than 70 voxels seem to be unrealistic, since their behavior significantly differs from the one of experimental sample no. 1 (analogue of virtual sample no. 13 in Table 4). It implies that isolated and highly branched Si clusters are hardly probable to occur in the material. Experimental sample no. 1 shows the highest strength.

### *3.3. Discussion*

The aim of this study is to describe and compare the influence of different Si morphologies on the mechanical behavior in a qualitative way that gives important information on how a high-strength structure should look like.

Therefore, to draw a conclusion on the results of FEM simulations, the following

is assumed: By comparing mechanical performances of different morphologies, one structure is regarded as more high-strength than the other if its simulated stress-strain curve is located above the other.

It is shown that the morphological variations generated by the stochastic model significantly influence the mechanical behavior at the microscale. A decrease of both external and internal competition parameters results in an increase in material strength. On the morphological level, it implies that there is more space for new Si branches to appear and to grow. After the dilation step of the model, neighboring branches can merge together, forming thereby new connections. Here, the connectivity of Si is evaluated by two parameters: The Euler number (Euler number density) and the volume fraction of the largest individual particle of Si relative to the total volume of Si within the bounding box, as in [25]. Fig. 10 shows the evolution of both characteristics with the external competition parameter. When  $t_{external}$  is decreasing, on the one hand, the Euler number turns negative and increases in the absolute value, which implies the presence of a network structure and, on the other hand, the volume fraction of the largest individual particle of Si approaches 100%, which indicates that most of the Si component within the bounding box is comprised in only one connected particle. The mechanical strength increases with the connectivity of Si, i.e. with a decreasing Euler number and an increasing volume fraction of the largest individual particle of Si (see Fig. 5 and Table 2).

However, Fig. 11 illustrates that the volume fraction of the largest individual particle ( $V_{MaxCluster}/V_{TotalSi}$ ) does not always reflect the connectivity changes.

Here, when  $t_{internal}$  is decreasing, the volume fraction of the largest individual

particle of Si does not change significantly, which gives the illusion that the connectivity and strength remain constant, although the material strength increases (see Fig. 7 and Table 3). At the same time, the Euler number increases by almost six times in absolute values and thus, indicates an increase in connectivity and material strength.

Where the connectivity is not concerned, for example, in the case of disjoint or simply connected structures that consist of disconnected Si particles, the number of the particles plays a significant role, i.e. the strength increases with the number of particles; however, it still remains below the strength of network structures.

The results of the present investigation fit the results obtained in [9] for an unmodified AlSi12 alloy; here, a strengthening effect of connected Si particles in an Al matrix has been presented. For Sr-modified Al-Si alloys, there is a balance between high strength and ductility. In [4], it has been shown that the modification of Al-Si alloys results in a moderated increase in strength while the increase in elongation is more significant. Thus, the ductility of the alloy is also highly affected by the effect of modification and the morphology of the microconstituents. An optimal microstructure is rather characterized by the moderated strength and high ductility. Indeed, disconnected particles of Si can much better accommodate stress through the deformation of the eutectic Al and the movement of Si particles relative to each other, while in connected particles, the same stress is more probable to cause damage. In order to deduce a morphological scenario of an optimal structure for Al-Si alloys and give a quantitative assessment, further investigations are required. Particularly, an

investigation of the fracture mechanism and a simulation of the fracture should be carried out.

#### **4. Conclusions and Outlook**

The correlation between the microstructure and the mechanical behavior of Al-Si alloys has been analyzed by combining a stochastic microstructure model of the eutectic Si in Al-Si alloys with FEM simulations. This in-silico approach using stochastic simulation models permits the generation of a large variety of synthetic 3D microstructures that reflect the mechanical properties of the eutectic and therefore are used to evaluate the mechanical strength of the alloy for different morphological scenarios. The stochastic model is controlled by parameters, such as the radius  $r_{cox}$  and the internal  $t_{internal}$  and external  $t_{external}$  competition parameters. Thus, by varying the model parameters, virtual Si structures, which differ from each other with respect to the number of Si particles, their branching, and connectivity, have been generated. Then, using FEM simulations, the mechanical behavior of different eutectic structures has been evaluated in terms of the mechanical strength. The following conclusions have been drawn:

- The strength of the material increases with the connectivity and the branching of the Si particles as well as with the number of particles for simply connected structures.
- The connectivity can be evaluated by means of the Euler number and the volume fraction of the largest individual particle of Si within the bounding box. However, the volume fraction of the largest individual particle alone is not sufficient to assess the connectivity changes or the changes in

strength. The Euler number is shown to be highly effective in characterizing the connectivity.

- The strength of the materials increases with decreasing the Euler number. The structures with similar values of the Euler number have a similar mechanical behavior. This tendency is observed for both virtual and experimental data. Therefore, the Euler number is a relative, yet effective measure of the strength in cases for which it is necessary to compare a performance of different structures without mechanical tests.
- This study demonstrates a promising methodology to find correlations between microstructure and functionality of the material and shows the feasibility and effectiveness of an approach that uses virtual tools, yet based on real data.

### **Acknowledgments**

The research was supported by funding from the German Federal Ministry of Economics and Technology within the project AiF 17204N. The authors would like to acknowledge the EU funding in the framework of the project AME-Lab (European Regional Development Fund C/4-EFRE-13/2009/Br).

### **References**

- [1] J. E. Gruzleski, B. M. Closset, *The Treatment of Liquid Aluminum-Silicon Alloys*, American Foundrymen's Society, Inc., Des Plaines, Illinois, 1990.
- [2] *Properties and Selection: Nonferrous Alloys and Special-Purpose Materials*, ASM Handbook, vol. 2, ASM International, 1990.
- [3] S. Hegde, K. Prabhu, *Modification of eutectic silicon in Al-Si alloys*, J.

- Mater. Sci. 43 (2008) 3009-3027.
- [4] N. Fat-Halla, Structural modification of Al-Si eutectic alloy by Sr and its effect on tensile and fracture characteristics, J. Mater. Sci. 24 (1989) 2488-2492.
- [5] M. M. Haque, Effects of strontium on the structure and properties of aluminium-silicon alloys, J. Mater. Process. Technol. 55 (1995) 193-198.
- [6] S.-S. Shin, E.-S. Kim, G.-Y. Yeom, J.-C. Lee, Modification effect of Sr on the microstructures and mechanical properties of Al–10.5Si–2.0Cu recycled alloy for die casting, Mater. Sci. Eng. A. 532 (2012) 151-157.
- [7] F. Lasagni, A. Lasagni, C. Holzapfel, F. Mücklich, H. P. Degischer, Three dimensional characterization of unmodified and Sr-modified Al-Si eutectics by FIB and FIB EDX tomography, Adv. Eng. Mater. 8 (2006) 719-723.
- [8] G. Requena, G. Garcés, M. Rodríguez, T. Pirling, P. Cloetens, 3D architecture and load partition in eutectic Al-Si alloys, Adv. Eng. Mater. 11 (2009) 1007-1014.
- [9] G. Requena, G. Garcés, Z. Asghar, E. Marks, P. Staron, P. Cloetens, The effect of the connectivity of rigid phases on strength of Al-Si alloys, Adv. Eng. Mater. 13 (2011) 674-684.
- [10] M. Sahoo, R. Smith, Mechanical properties of unidirectionally solidified Al-Si eutectic alloys, Met. Sci. J. 9 (1975) 217-222.
- [11] A. Saigal, E. R. Fuller Jr., Analysis of stresses in aluminum-silicon alloys, Comp. Mater. Sci. 21 (2001) 149-158.
- [12] N. Raghukiran, A. K. Mohamed, R. Kumar, Study of the Influence of Silicon

Phase Morphology on the Microstructural Stress Distribution in Al–Si Alloys Using Object Oriented Finite Element Modeling, *Adv. Eng. Mater.* 15 (2013) 1-10.

- [13] J. Ohser, F. Mücklich, *Statistical Analysis of Microstructures in Materials Science*, J. Wiley & Sons, Chichester, 2000.
- [14] F. Lasagni, A. Lasagni, E. Marks, C. Holzapfel, F. Mücklich, H. P. Degischer, Three-dimensional characterization of 'as-cast' and solution-treated AlSi12(Sr) alloys by high-resolution FIB tomography, *Acta Mater.* 55 (2007) 3875-3882.
- [15] G. Gaiselmann, O. Stenzel, A. Kruglova, F. Mücklich, V. Schmidt, Competitive stochastic growth model for the 3D morphology of eutectic Si in Al-Si alloys, *Comp. Mater. Sci.* 69 (2013) 289-298.
- [16] G. Gaiselmann, M. Neumann, O. Pecho, T. Hocker, V. Schmidt, L. Holzer, Quantitative relationships between microstructure and effective transport properties based on virtual materials testing, *AIChE J.* 60 (2014) 1983-1999.
- [17] V. Schmidt, G. Gaiselmann, O. Stenzel, Stochastic 3D models for the micro-structure of advanced functional materials, in: V. Schmidt (Ed.), *Stochastic Geometry, Spatial Statistics and Random Fields: Models and Algorithms. Lecture Notes in Mathematics*, Springer, 2015, pp. 95-141.
- [18] M. Roland, A. Kruglova, G. Gaiselmann, T. Brereton, V. Schmidt, F. Mücklich, S. Diebels, Numerical simulation and comparison of a real Al-Si alloy with virtually generated alloys, *Arch. Appl. Mech.*, Springer-Verlag

Berlin Heidelberg, 2014.

- [19] M. Roland, A. Kruglova, N. Harste, F. Mücklich, S. Diebels, Numerical simulation of Al-Si alloys with and without a directional solidification, *Image Anal Stereol.* 33 (2014) 29-37.
- [20] COMSOL, COMSOL Multiphysics User's Guide, Version 4.3b, 2010.
- [21] R. Hill, *The Mathematical Theory of Plasticity*, Oxford University Press, New York, 1998.
- [22] MAVI - Modular Algorithms for Volume Images, Fraunhofer Institute for Industrial Mathematics ITWM, [Online]. Available: <http://www.itwm.fraunhofer.de/en/departments/image-processing/microstructure-analysis/mavi.html>. [Accessed 03 02 2015]
- [23] Fiji Is Just ImageJ, [Online]. Available: <http://fiji.sc/Fiji>. [Accessed 03 02 2015]
- [24] J. C. Russ, R. T. Dehoff, *Practical Stereology*, Kluwer Academic/Plenum Publishers, New York, 2000.
- [25] D. Tolnai, G. Requena, P. Cloetens, J. Lendvai, H. P. Degischer, Effect of solution heat treatment on the internal architecture and compressive strength of an AlMg4.7Si8 alloy, *Mater. Sci. Eng. A.* 585 (2013) 480-487.

## Figure Captions

**Fig. 1.** 3D Si morphology in Al-Si alloys obtained by directional solidification in the bounding box of the size  $36.6 \mu\text{m} \times 16.8 \mu\text{m} \times 34.7 \mu\text{m}$  (a) and by die casting in the bounding box of the size  $19.4 \mu\text{m} \times 12.9 \mu\text{m} \times 19.4 \mu\text{m}$  (b).

Different colors represent disconnected particles of Si, Al matrix is transparent.

The first sample (experimental sample no. 1) consists of many disconnected Si particles. The second sample (experimental sample no. 2) comprises a large connected Si particle.

**Fig. 2.** Schematic representation of the competitive stochastic growth model and the parameters of the model, such as an external ( $t_{external}$ ) and internal ( $t_{internal}$ ) competition parameters and a hardcore radius ( $r_{cox}$ ).

**Fig. 3.** Reconstruction of coral-like Si particles within Al-Si eutectic obtained by FIB/SEM tomography (a); a realization derived from the competitive stochastic growth model that was fitted to the experimental data (b) (different colors represent disconnected particles).

**Fig. 4.** 3D images of simulation of eutectic Si with  $t_{external} = 0.1$  voxels (a) and  $t_{external} = 40$  voxels (b);  $t_{internal}$  is set to 30 voxels. When decreasing the external competition parameter  $t_{external}$ , a highly connected structure or network of the Si component is formed.

**Fig. 5.** Finite element simulations on virtual structures with various external competition parameters and on two experimental samples: strength of the material increases with the connectivity of Si (i.e. with a decreasing  $t_{external}$  for virtual samples).

**Fig. 6.** 3D images of virtual microstructures of eutectic Si with  $t_{internal} = 10$  voxels (a) and  $t_{internal} = 30$  voxels (b);  $t_{external}$  is 5 voxels. When decreasing the internal competition parameter  $t_{internal}$ , a highly connected and branched structure of the Si component is formed.

**Fig. 7.** Finite element simulations on structures with various internal competition parameters and on two experimental samples: strength of the material increases with the connectivity and the branching of Si (i.e. with a decreasing  $t_{internal}$  for virtual microstructures).

**Fig. 8.** 3D image of simulation of eutectic Si with  $r_{cox} = 120$  voxels. When the parameter  $r_{cox}$  increases, the number of particles decreases while their branching increases.

**Fig. 9.** Finite element simulations on structures with various values of  $r_{cox}$  and on experimental sample no. 1: strength of the material increases with the number of particles (i.e. with a decreasing  $r_{cox}$  for virtual microstructures).

**Fig. 10.** Evolution of the Euler number and the volume fraction of the largest individual particle of Si via the external competition parameter: both parameters reflect the connectivity changes.

**Fig. 11.** Evolution of the Euler number and the volume fraction of the largest individual particle of Si via the internal competition parameter: only the Euler number reflects the connectivity changes.

- The correlation between Si connectivity and strength of the material is analyzed by means of the stochastic model and FEM simulations.
- The strength of the material increases with the connectivity and the branching of Si particles as well as with the number of particles for simply connected structures.
- The Euler number is shown to be highly effective in characterizing the connectivity.
- Feasibility and effectiveness of an approach that uses virtual, yet based on real data tools, to study structure-properties correlations is demonstrated.

Table 1

Chemical composition, casting procedure, and Euler number density of the experimental Al-Si alloys.

Sample	Composition (wt. %)	Casting procedure	Euler number density ( $m^{-3}$ )
experimental sample no. 1	7% Si, 0.015% Sr	directional solidification	$4.80 \times 10^{14}$
experimental sample no. 2	7% Si, 0.3% Mg, 0.02% Sr	die casting	$-2.61 \times 10^{17}$

Table 2

Morphological properties of virtual microstructures generated by varying the external competition parameter  $t_{external}$ . With decreasing  $t_{external}$ , the volume fraction of the largest individual particle of Si ( $V_{MaxCluster}/V_{TotalSi}$ ) increases while the Euler number gets negative and decreases; both indicate an increase in the connectivity of Si.

Sample	$t_{external}$	Number of particles	$V_{MaxCluster}/V_{TotalSi}$	Euler number density ( $m^{-3}$ )	Euler number	Number of branches
sample no. 1	40	222	3	80	$5.55 \times 10^{15}$	1006
sample no. 2	20	178	7	-117	$-8.12 \times 10^{15}$	2064
sample no. 3	10	96	66	-425	$-2.95 \times 10^{16}$	3420
sample no. 4	5	79	90	-699	$-4.85 \times 10^{16}$	4650
sample no. 5	0.1	81	98	-1296	$-9.00 \times 10^{16}$	6725

Table 3

Morphological properties of virtual microstructures generated by changing the internal competition parameter  $t_{internal}$ . With decreasing  $t_{internal}$ , the volume fraction of the

largest individual particle of Si ( $V_{MaxCluster}/V_{TotalSi}$ ) slightly increases while the Euler number decreases; both indicate an increase in the connectivity of Si.

Sample	$t_{internal}$	Number of particles	$V_{MaxCluster}/V_{TotalSi}$	Euler number	Euler number density ( $m^{-3}$ )	Number of branches
sample no. 4	30	79	90	-699	$-4.85 \times 10^{16}$	4650
sample no. 6	25	77	94	-764	$-5.30 \times 10^{16}$	4925
sample no. 7	20	79	97	-981	$-6.81 \times 10^{16}$	5730
sample no. 8	15	93	96	-1965	$-1.36 \times 10^{17}$	9244
sample no. 9	10	131	98	-4151	$-2.88 \times 10^{17}$	14347

Table 4

Morphological properties of virtual microstructures generated by varying values of  $r_{cox}$ . With increasing  $r_{cox}$ , the number of particles decreases while the number of branches per particle increases. The connectivity and the volume fraction of the largest individual particle of Si ( $V_{MaxCluster}/V_{TotalSi}$ ) undergo only minor changes. The connectivity is computed by subtracting the Euler number from the number of Si clusters.

Sample	$r_{cox}$	Number of particles	$V_{MaxCluster}/V_{TotalSi}$	Connectivity	Number of branches
sample no. 10	120	69	7	195	1411
sample no. 11	70	130	3	159	1158
sample no. 12	60	162	2	137	1200
sample no. 13	55	211	2	144	1683

Figure 1a  
[Click here to download high resolution image](#)

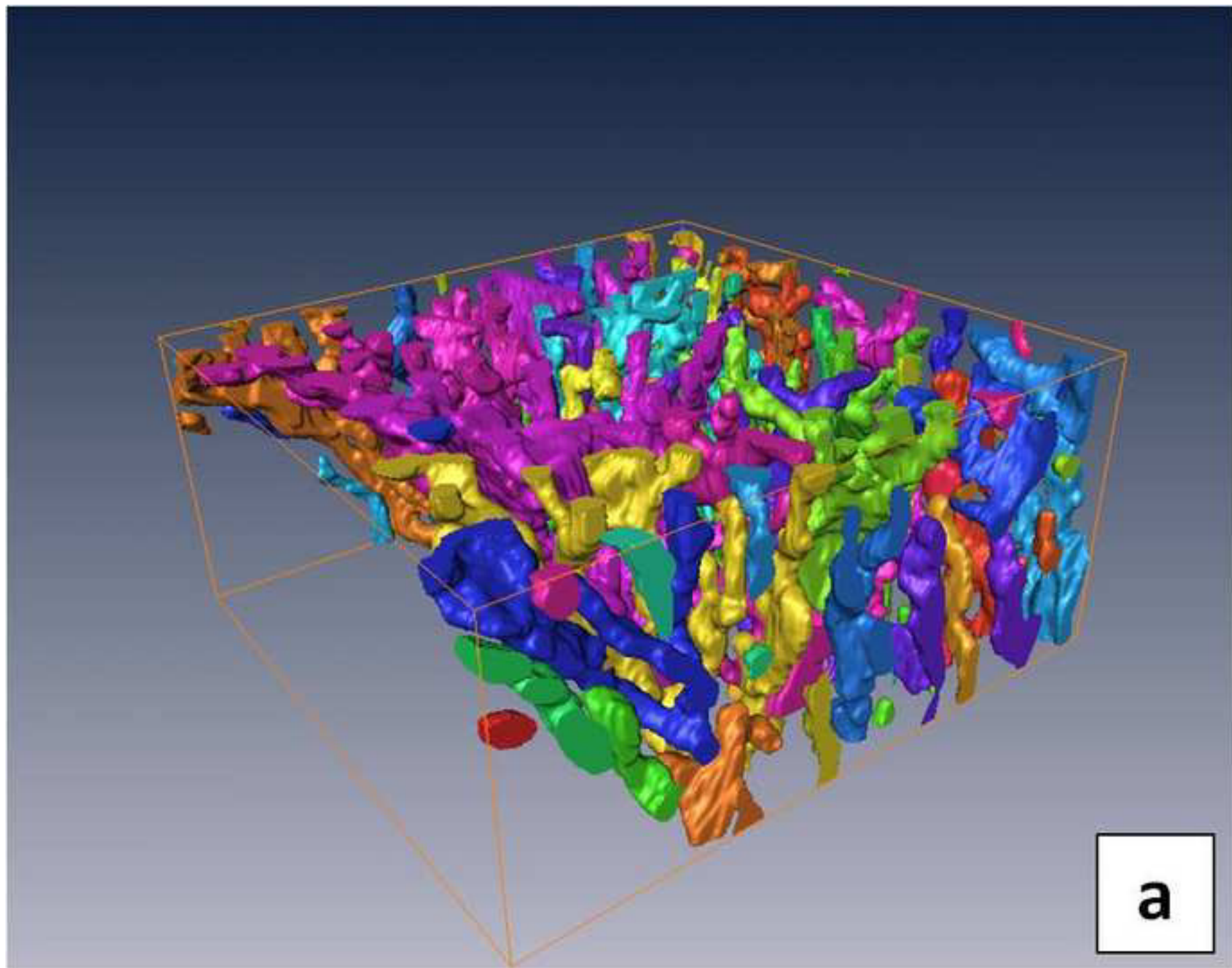


Figure 1b  
[Click here to download high resolution image](#)

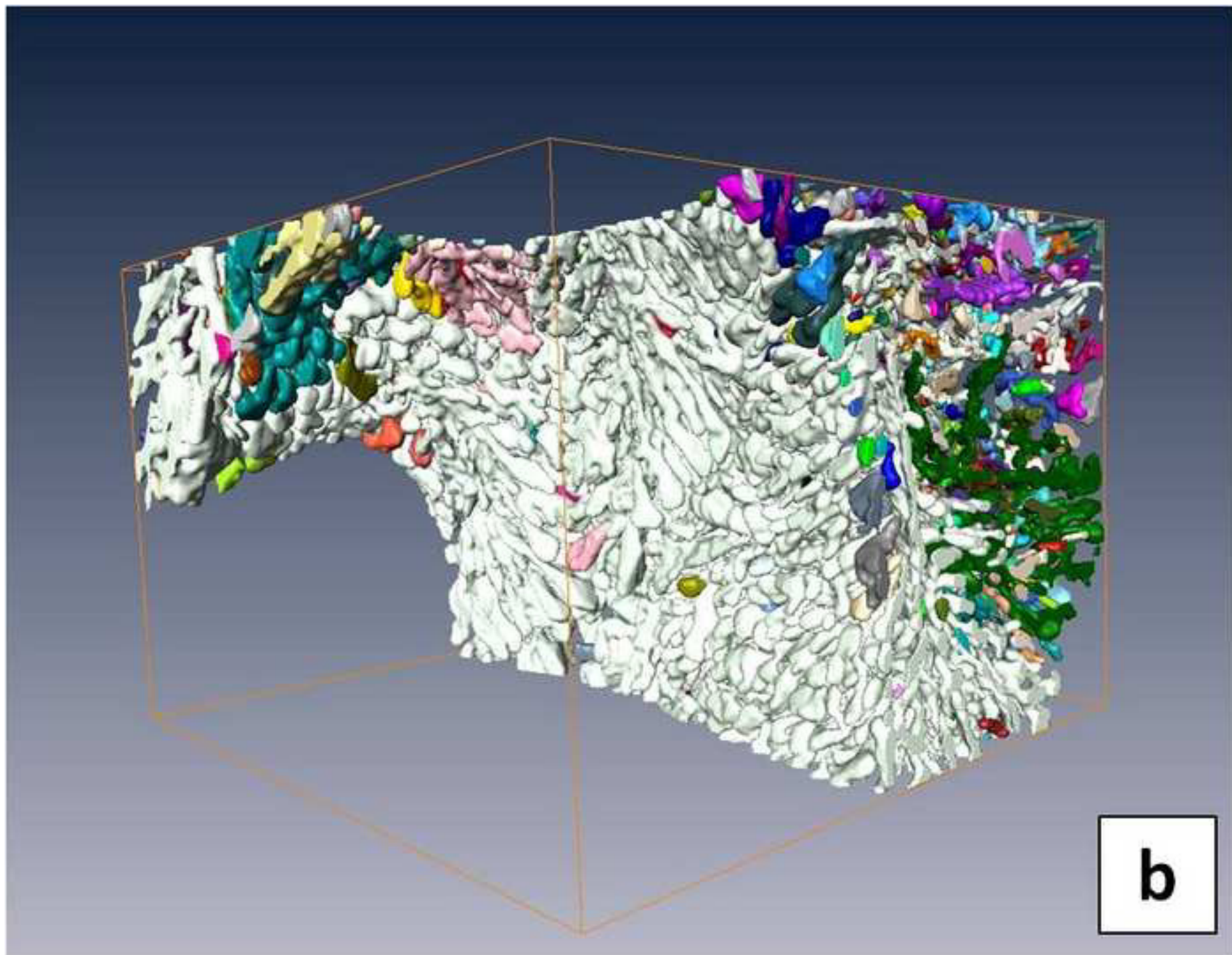


Figure 2  
[Click here to download high resolution image](#)

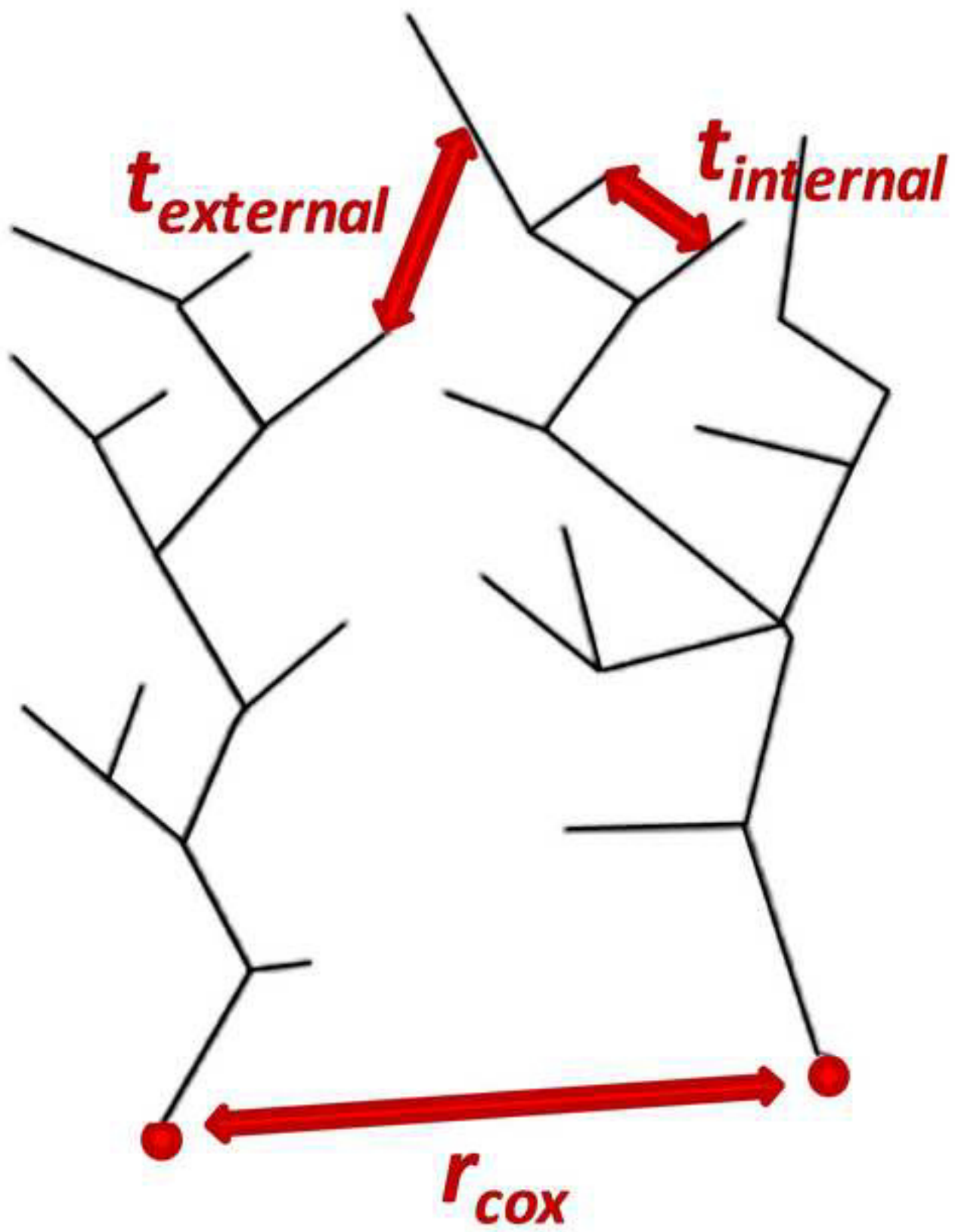


Figure 3a  
[Click here to download high resolution image](#)

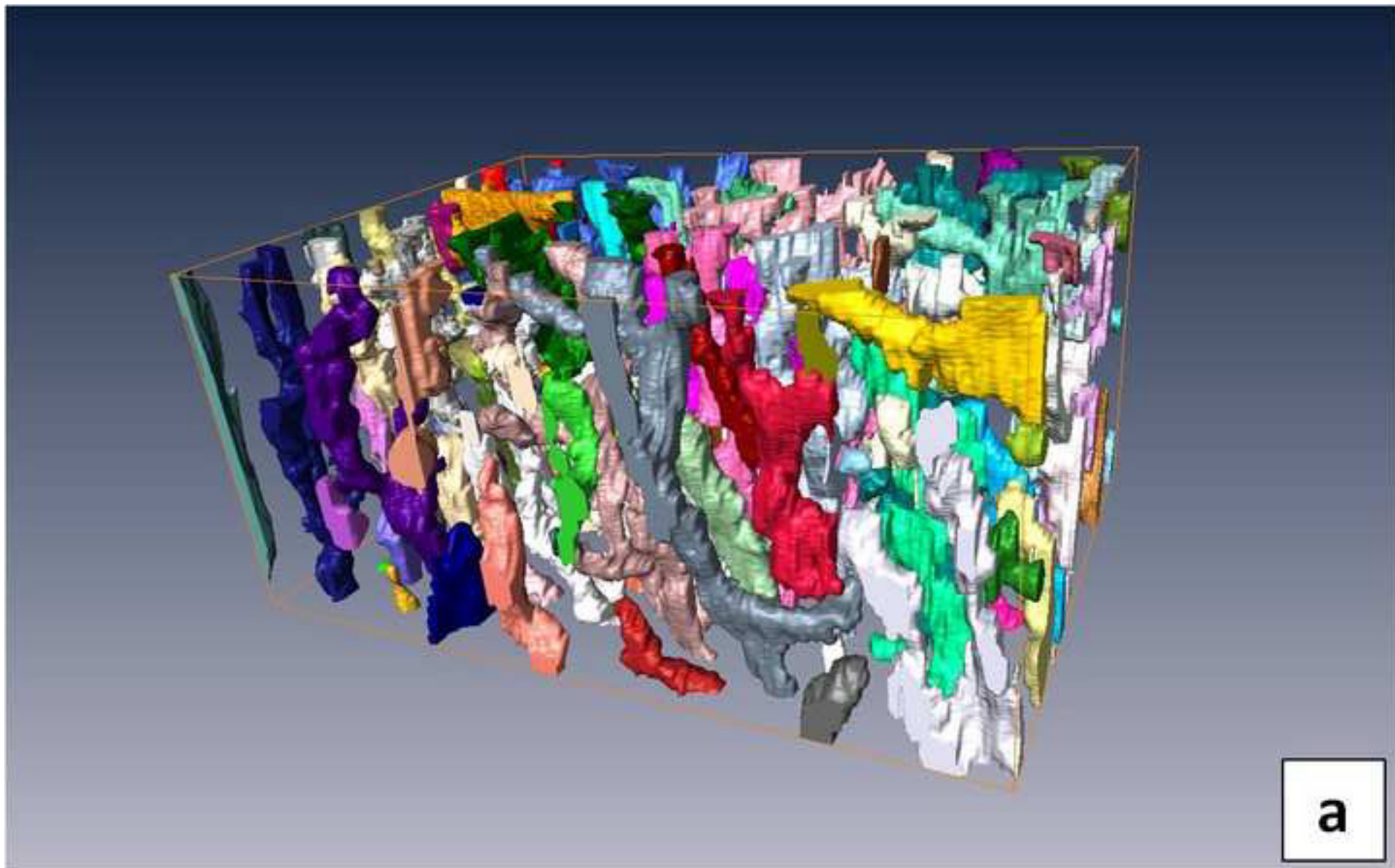


Figure 3b  
[Click here to download high resolution image](#)

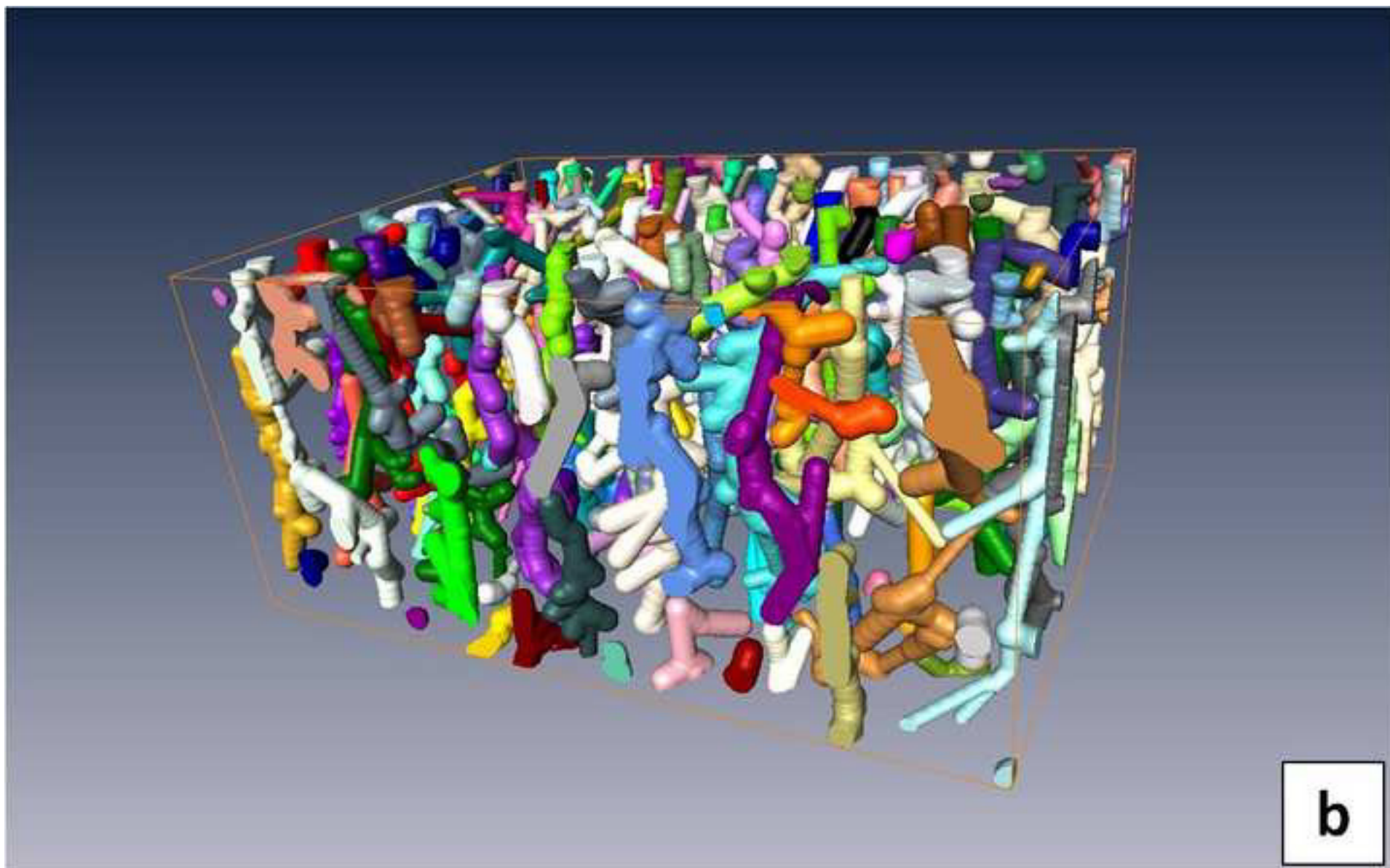


Figure 4a  
[Click here to download high resolution image](#)

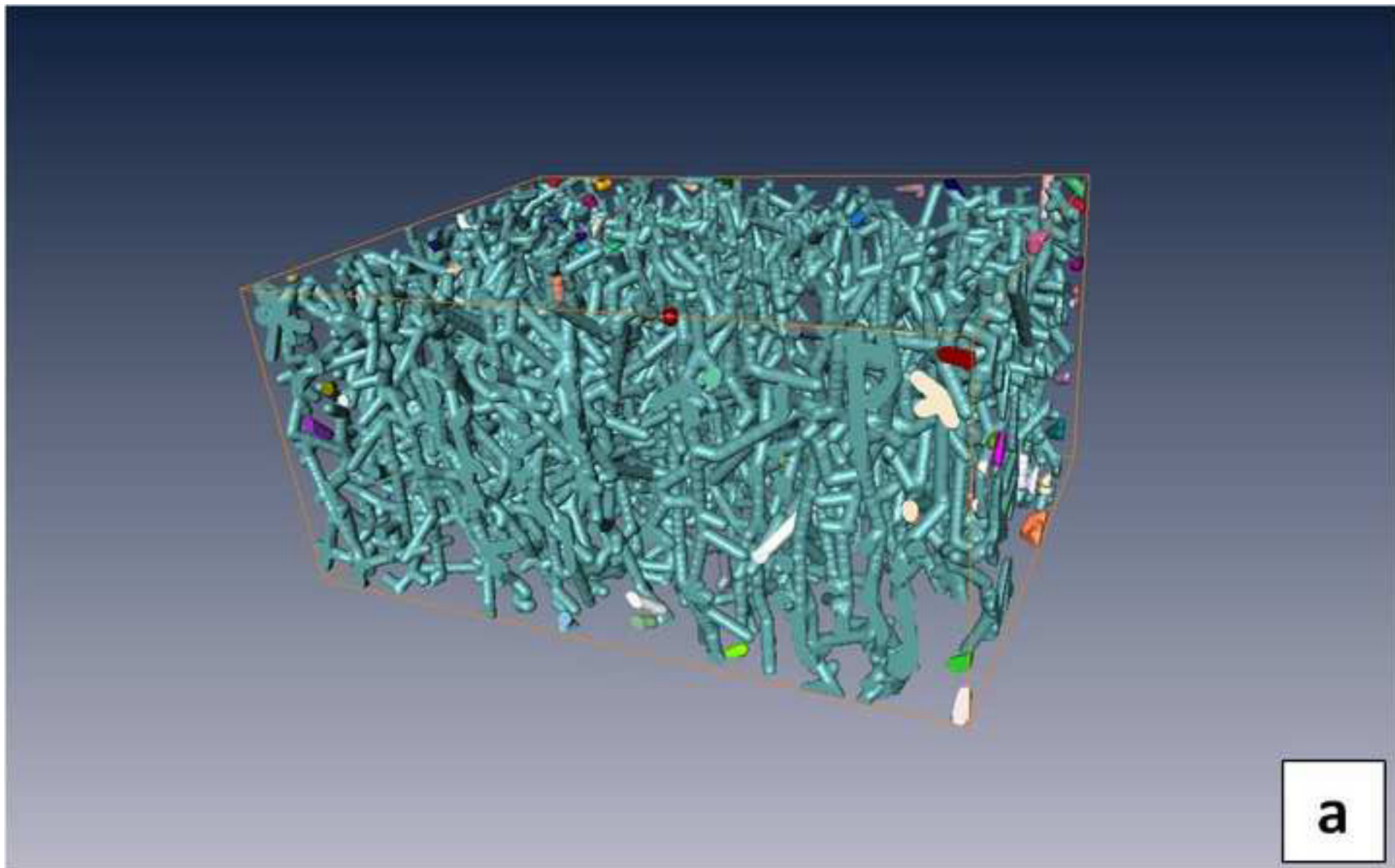


Figure 4b  
[Click here to download high resolution image](#)

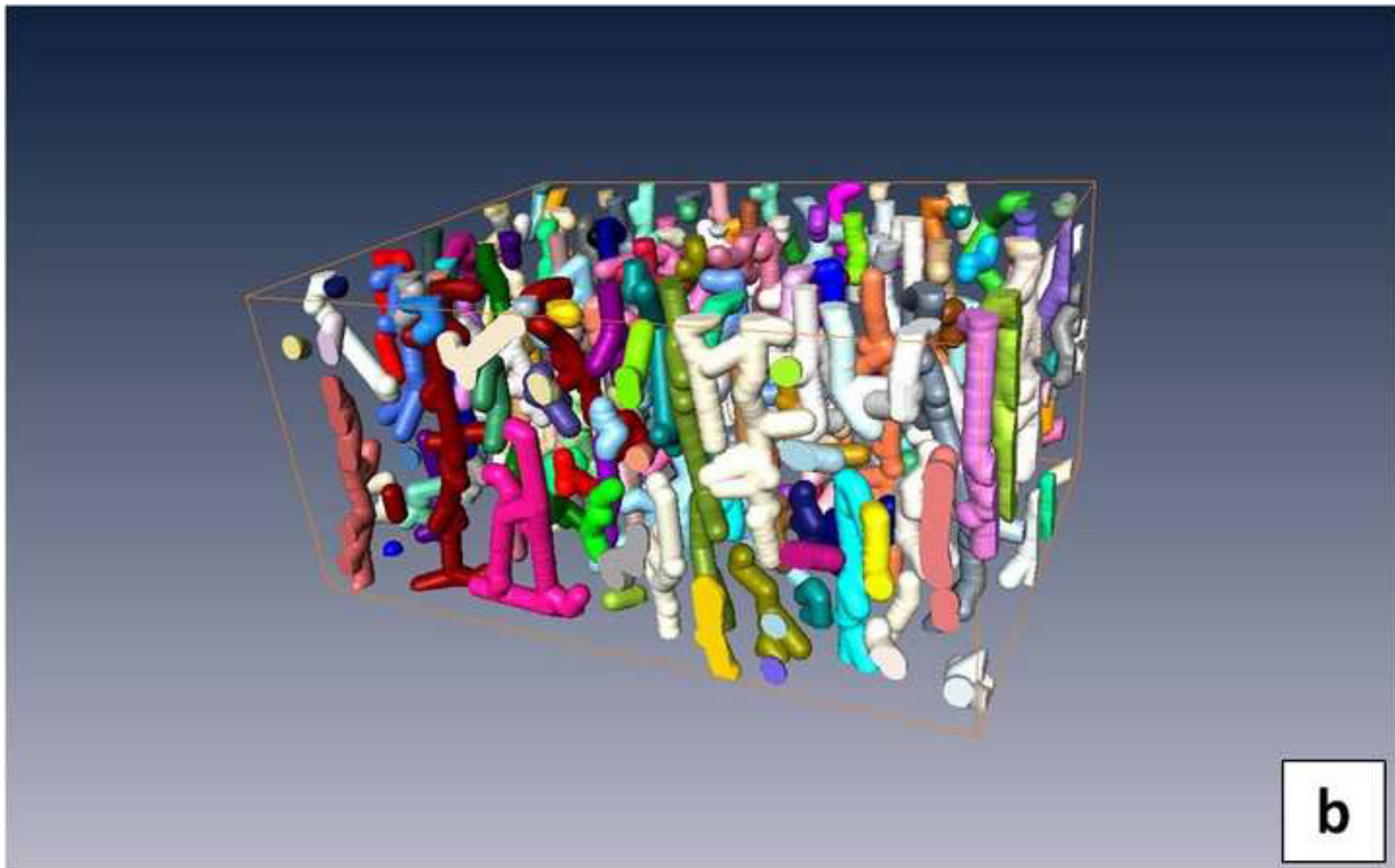


Figure 5  
[Click here to download high resolution image](#)

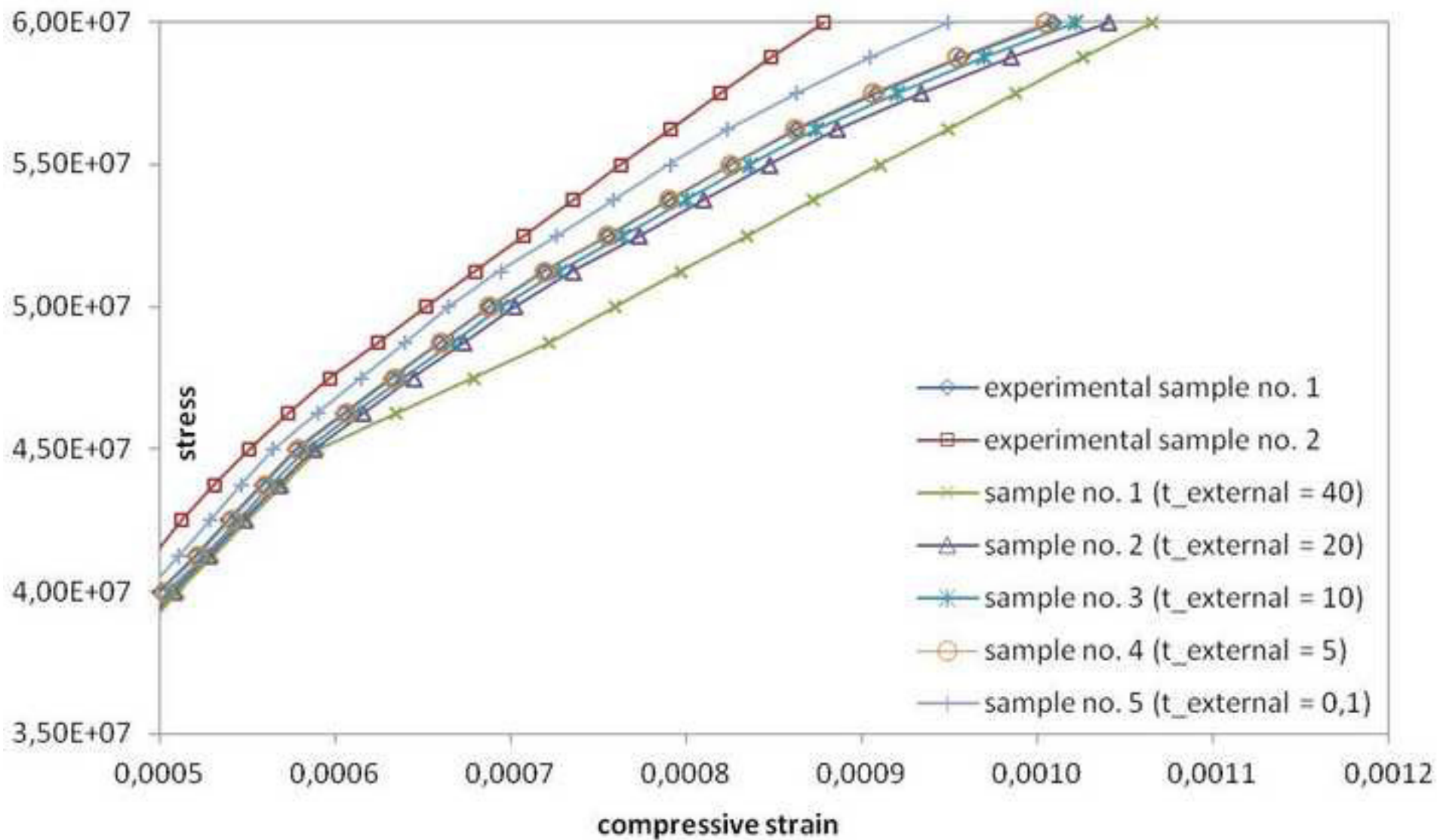


Figure 6a  
[Click here to download high resolution image](#)

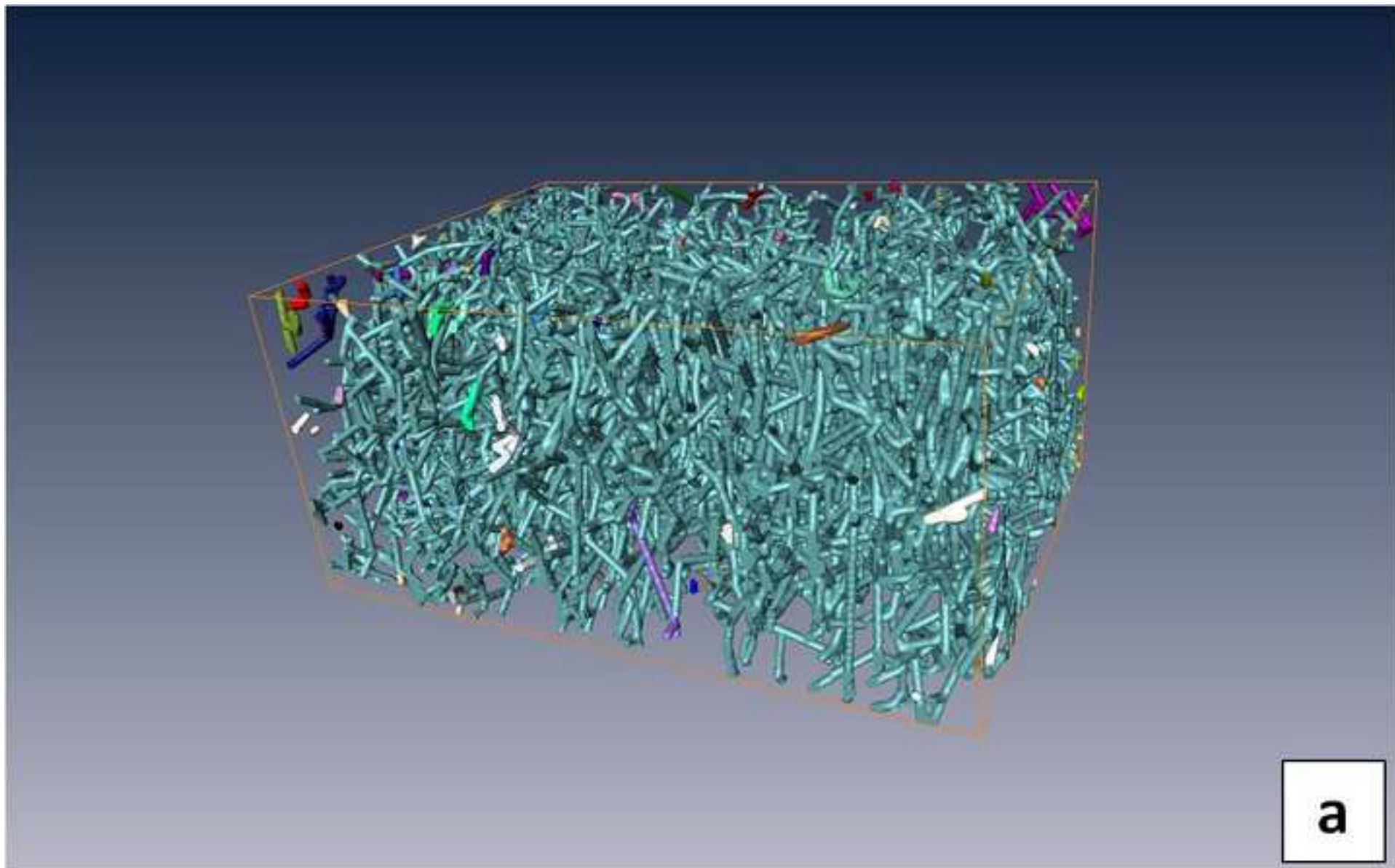


Figure 6b  
[Click here to download high resolution image](#)

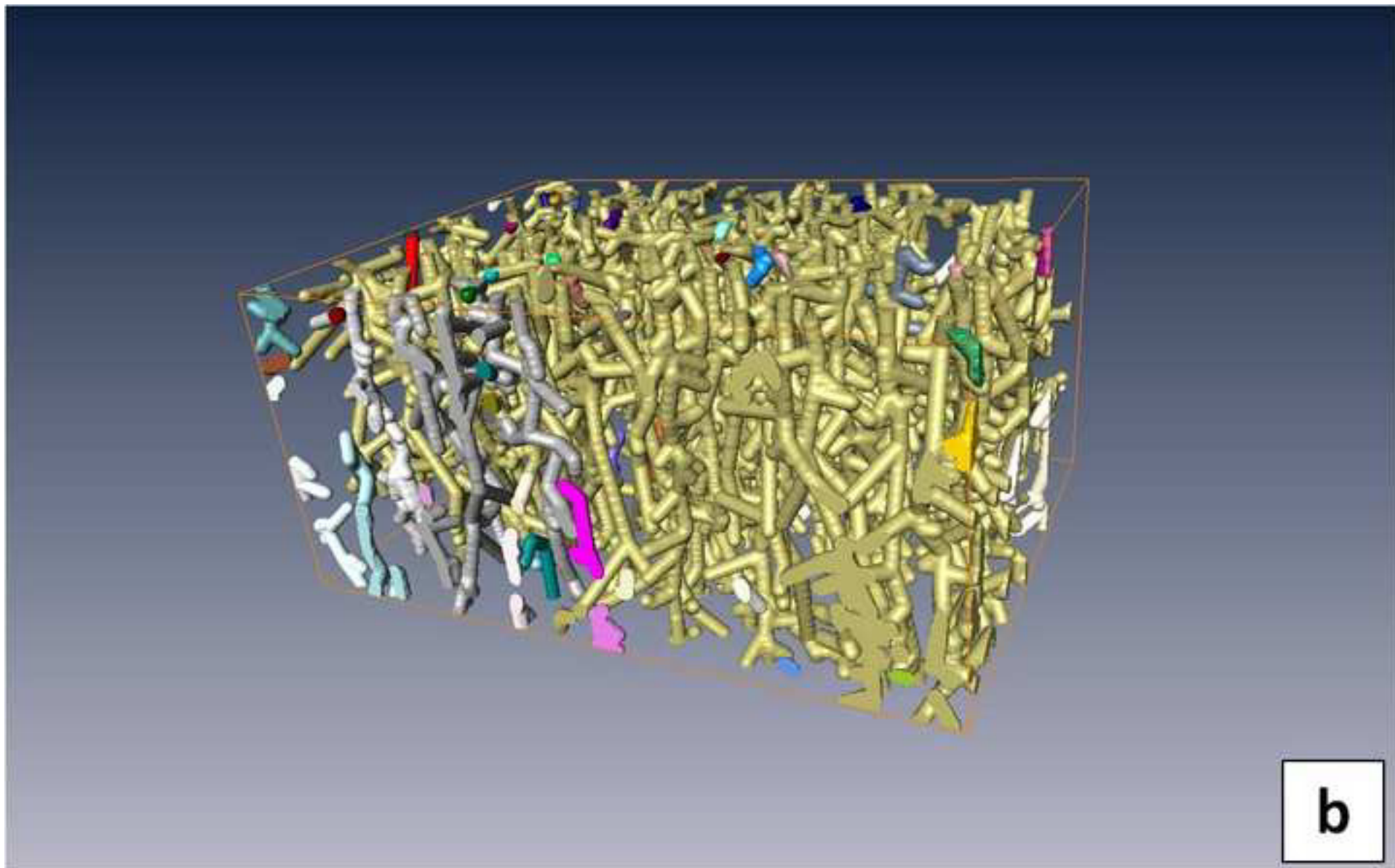




Figure 8  
[Click here to download high resolution image](#)

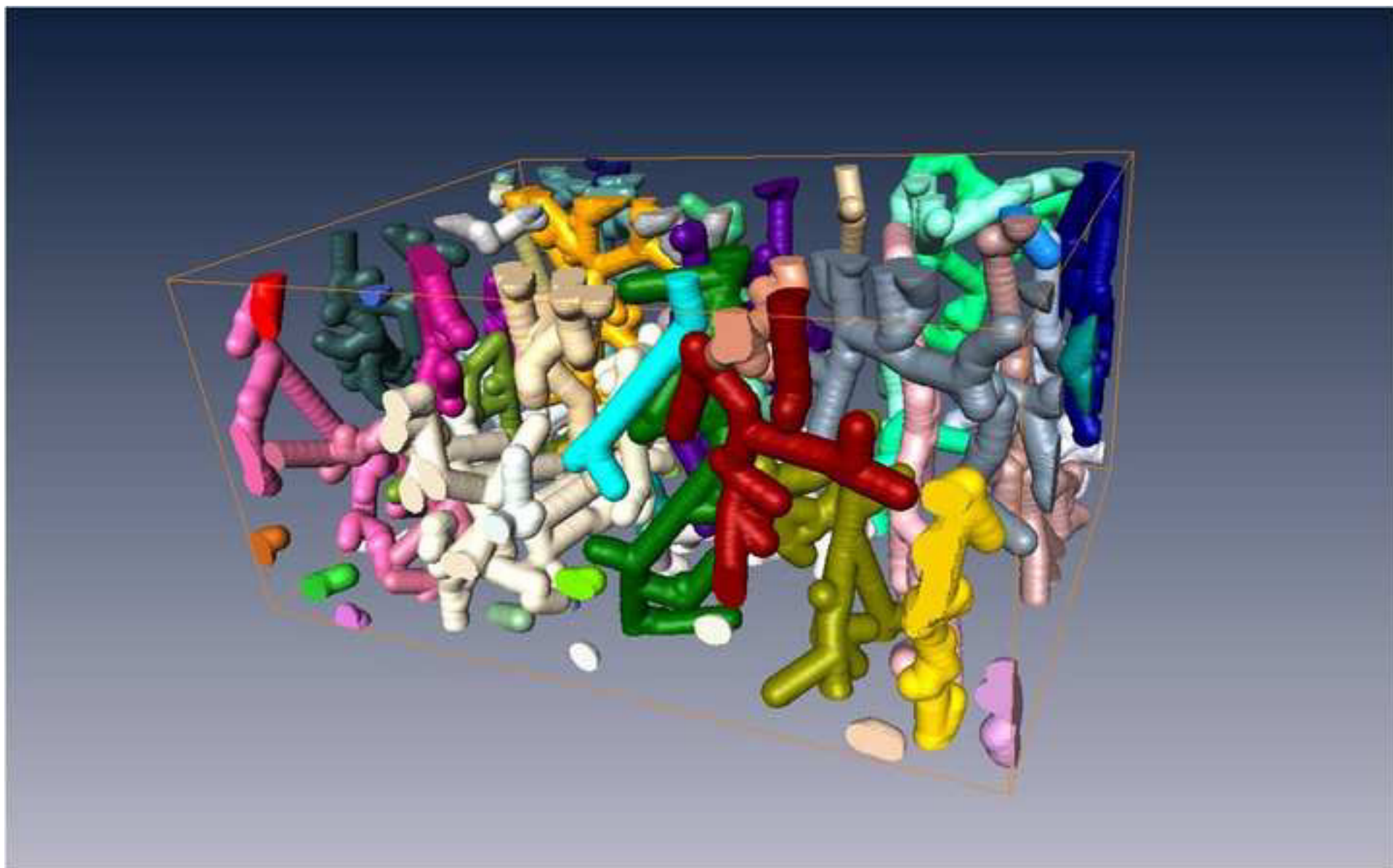


Figure 9  
[Click here to download high resolution image](#)

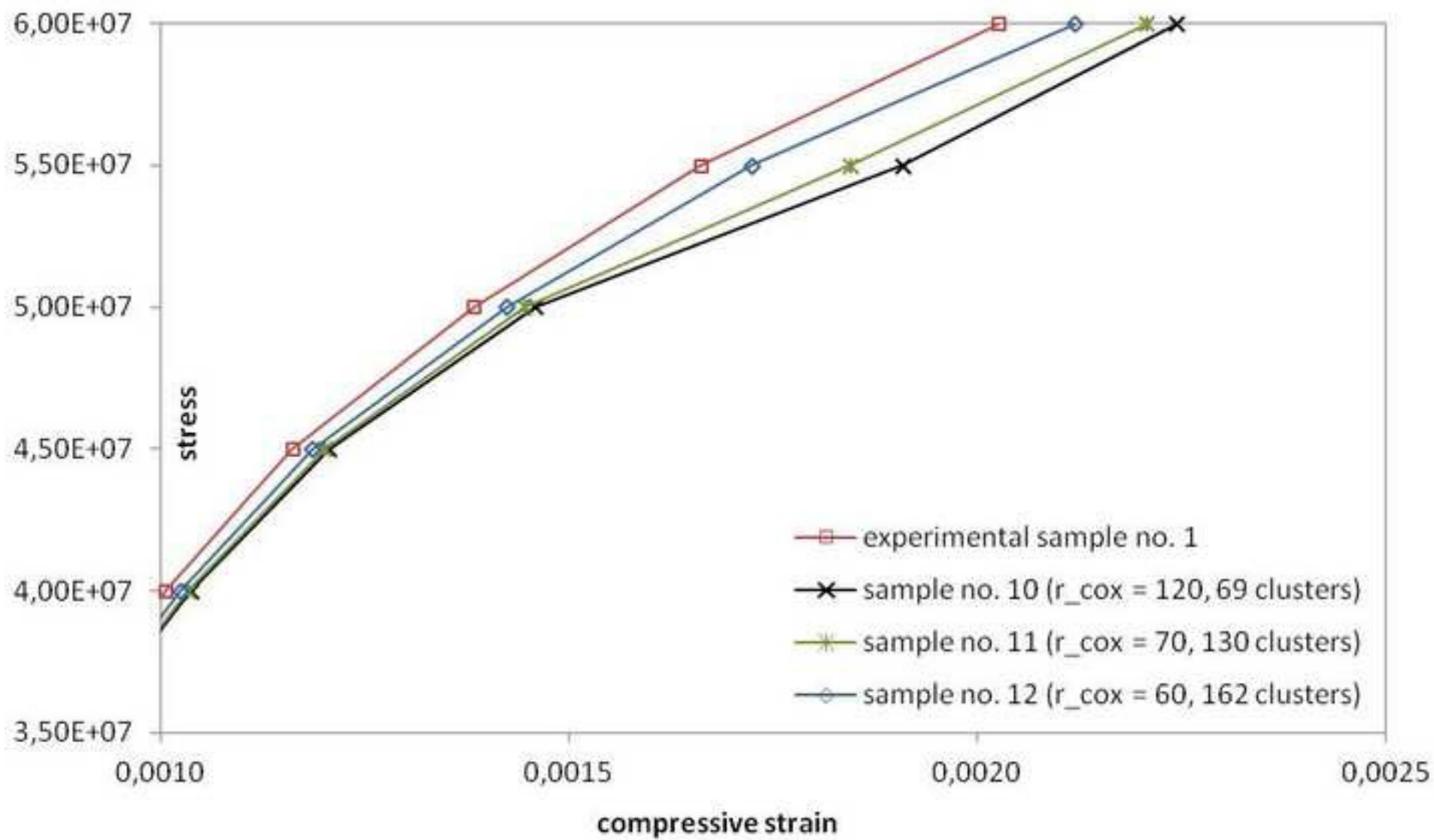


Figure 10  
[Click here to download high resolution image](#)

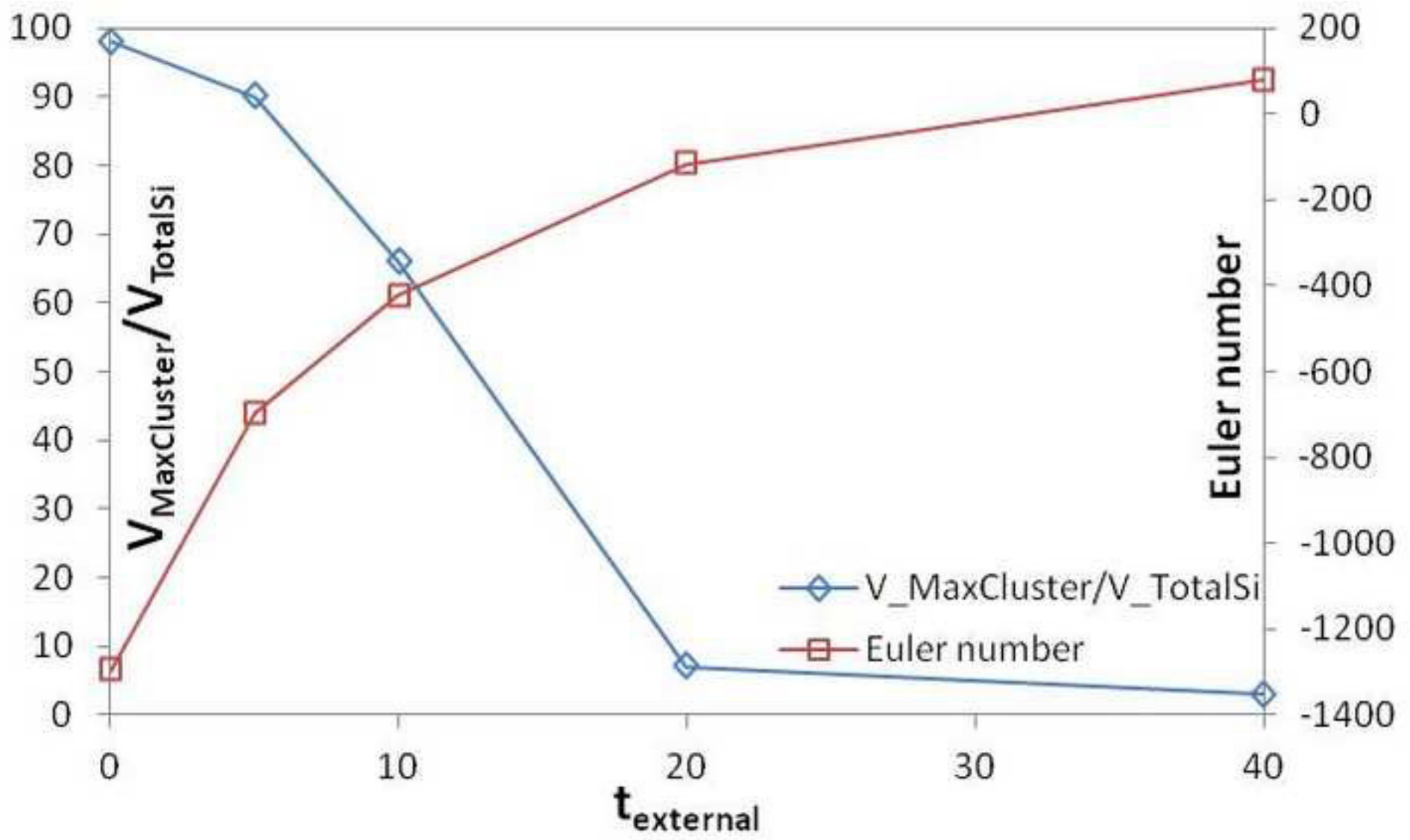


Figure 11  
[Click here to download high resolution image](#)

